Evaluation of parallel transmit RF-shimming performance for 3 tesla whole-body imaging

F. Wiesinger[1], G. McKinnon[2], D. Lange[1], M. Vogel[1], E. Boskamp[2], L. Blawat[2], M. Menzel[1], W. Loew[1], H. Koenig[1], Y. Zhu[3], and P. Gross[1]

[1]Imaging Technologies, GE Global Research Europe, Munich, Germany, [2]Applied Science Lab, GE Healthcare, Waukesha, WI, United States, [3]Imaging Technologies, GE Global Research, Niskayuna, NY, United States

INTRODUCTION: Over the past decade methodological breakthroughs as well as solid technical engineering work have introduced 3 tesla high field MR into clinical practice. Nevertheless, high field systems still pose challenges in terms of RF excitation uniformity (i.e. RF-shading) and specific absorption rate (SAR) limitations. In particular, RF wave interference effects can lead to inconsistent contrast behavior and in extreme cases even to complete signal cancellation. From the intrinsic subject dependence of RF shading it is clear that coil-only based approaches principally cannot solve this problem for the general case. Recently introduced parallel transmit technologies with enhanced control over the excitation process are considered as one potential solution for these problems. Two different flavors of parallel transmit are distinguished [1]: 1.) (static) RF-shimming: In this case each transmit pathway has the flexibility to add a complex weighting to an otherwise constant RF-waveform. 2.) Dynamic RF-shimming (full parallel transmit): Here each transmit path has its own fully independent RF-excitation capability. The scope of this work was to evaluate two static RF-shimming implementations against conventional quadrature excitation for 3 tesla, whole-body imaging.

MATERIALS and METHODS: In order to perform static RF-shimming on a clinical GE Signa Excite 3T scanner (GE Healthcare, Milwaukee, WI) following two hardware modifications have been implemented [2]: 1.) A multi-channel controller box divides the RF-waveform coming from the RF-exciter in up to eight independent sub-pathways. Separate computer controlled attenuators and phase shifters permit independent complex weighting of the otherwise identical RF-waveforms. 2.) As the RF-shimming adjustments occur before the power amplification stage, separate RF-amplifiers have to be added for each transmit pathway.

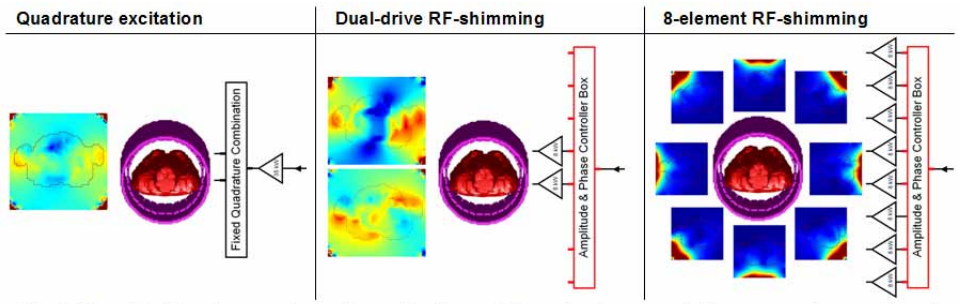

Fig.1: Simplified hardware schematics of the three different volume excitation concepts considered. Additionally corresponding $B_{1+}(\mathbf{r})$ maps are shown as obtained from FDTD simulations.

Following two static RF-shimming concepts have been implemented (cf. Fig. 1): 1.) *Dual-drive RF-shimming:* In this case the two independent modes of a birdcage coil are driven independently. While under ideal quasi-static conditions (i.e. low B_0 and/or object size) both birdcage modes have uniform B_{1+} distributions, at high B_0 and/or object size (with RF-wavelength effects coming into play) the modes get increasingly distinct, thereby introducing independent degrees of freedom for RF-shimming. 2.) *8-element RF-shimming:* For this purpose a dedicated whole-body transmit array (eight rectangular coil elements 19x56cm^2, inner diameter 61.4cm) has been installed [3]. The optimal set of RF-shimming weights $\{w_i\}$ was calculated by minimizing the deviation from the desired excitation profile B_{1+}^{des} (i.e. desired flip angle) over a user-defined region-of-interest (ROI). Taking the absolute value of the combined B_{1+} profile effectively removes the phase constraint and thereby significantly improves the obtained B_{1+} uniformity [Eq.1]. Besides RF-homogeneity, SAR measures could, in principal, also be included into the optimization.

$$\min_{w_1,\ldots,w_N} \int_{ROI} d\mathbf{r} \left[\left| \sum_{i=1,\ldots,N} w_i B_i^{1+}(\mathbf{r}) \right| - B_{des.}^{1+} \right]^2 \qquad [1]$$

RESULTS and DISCUSSION: For simulation purposes geometrically accurate FDTD models have been created for both the birdcage coil and the 8-element transmit array and been solved for the case of inhomogeneous (visible man) human body loading. Fig. 2 shows corresponding RF-shimming simulations for quadrature excitation versus dual-drive, and 8-element RF-shimming at a generally challenging slice location in the torso region. The standard deviations of the normalized B_{1+} histograms clearly illustrate the improvement of RF-uniformity with increasing RF-shimming flexibility. Measurements have been performed on a torso shaped elliptical phantom (long axis 40cm, short axis 26cm, length 48cm) with a cylindrical hole (diameter 20cm). The large phantom size together with the distilled (i.e. lossless) water filling resulted in significant wave interference effects and made this phantom to a challenging RF-shimming test case. Fig. 3 shows B_{1+} maps obtained for three considered excitation concepts. Application of RF-shimming again significantly improved B_{1+} uniformity. This example clearly demonstrates the additional benefit of having an 8 element transmit array.
This investigation demonstrates the potential of static RF-shimming for significant RF-shading reduction in whole-body, 3 tesla imaging. The required hardware extensions of the presented implementation include a multi-channel controller box, plus separate RF-amplifiers for each independent transmit coil element. It's important to note, that because of the B_{1+} superposition during the actual excitation process, this does not necessarily translates into an increase of required net RF power amplification capabilities. In order to make RF-shimming practicable for clinical routine further highly-efficient volumetric B_{1+} mapping techniques are required. Conceptually, it is clear that dynamic RF-shimming, with fully independent RF-waveform generation capabilities ultimately provides the more flexible solution for both RF-shading and SAR power limitations at high field.

References: [1] Katscher U, et al, ISMRM 2005: p. 2256; [2] Vogel MW, et al, ISMRM 2006: p3551; [3] Boskamp E, et al, ISMRM 2007: submitted.
Acknowledgement: This project receives co-funding under the Bavarian research initiative "Leading Edge Medical Technology Programs.

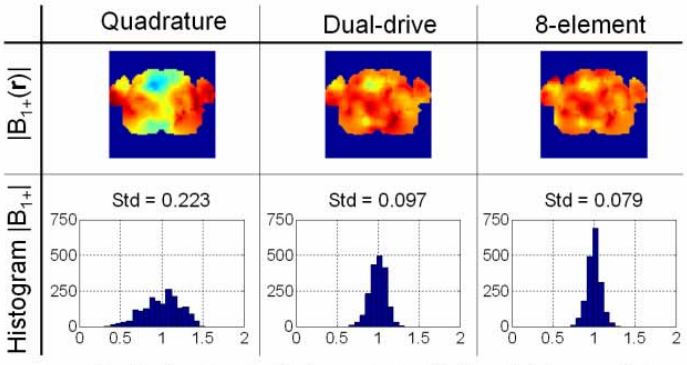

Fig. 2: RF-shimming for human body FDTD model (torso-region)

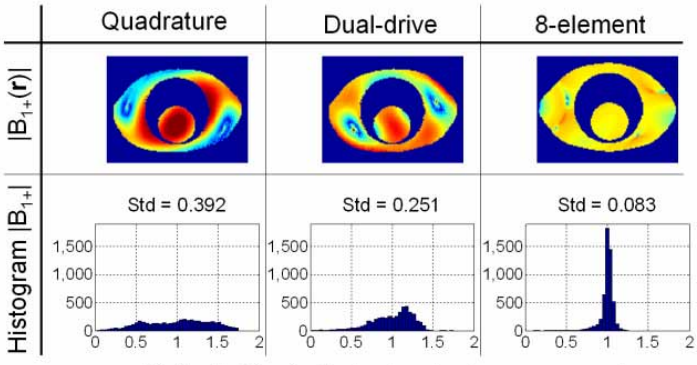

Fig.3: RF-shimming for lossless phantom measurements.